5-12-2020

Examining the Effect of El Nino Phenomena and Pacific Sea Surface Temperature on the Climate of the Glacierized White Mountains in Peru

Emily Reardon
Bridgewater State University

Examining the Effect of El Nino Phenomena and Pacific Sea Surface Temperature on the Climate of the Glacierized White Mountains in Peru

Emily Reardon

Submitted in Partial Completion of the
Requirements for Departmental Honors in Physics

Bridgewater State University

May 12, 2020

Dr. Robert Hellstrom, Thesis Advisor
Dr. Thomas Kling, Committee Member
Dr. Jeffrey Williams, Committee Member

Examining the Effect of El Nino Phenomena and Pacific Sea Surface Temperature on the Climate of the Glacierized White Mountains in Peru

Emily Reardon, Mentor Dr. Hellström

Physics Department
Bridgewater State University, MA

May 12, 2020

Abstract

The purpose of this study is to determine if there is a correlation between the El Niño Southern Oscillation, sea surface temperatures (SST) and the climate of the Rio Santa Basin. This study is an important step in understanding the dynamics of the glaciers as a critical control on hydrological features in alpine Andes Valleys. Temperature and precipitation measurements pulled from ground based weather stations in the Rio Santa drainage basin were aggregated, synchronized, and correlated with the changes in the Pacific ocean SST off the coast of Peru and into the central Pacific. The expectation is that we will see a significant correlation between the changing temperatures in the ocean in response to the ENSO events and the measurable changes in the valley but with a dependence on elevation as we rise from sea level to 4500 meters. The anticipated outcome would mean that changes in the ocean can affect long term and short-term atmospheric processes and mass balance of glaciers. Glaciers are critical for water resources of the Peruvian Andes, supplying agricultural, hydroelectric and everyday needs of hundreds of thousands of natives of Peru. These people rely on the steady flow of water from the mountain glaciers, especially during the 6-month dry season.

1 Background

1.1 Introduction to ENSO

Atmospheric circulation is a complex and dynamic system. It is not easily understood nor predicted. These systems have chaotic patterns which use a fixed and distinct set of rules for pattern formation, but remain unpredictable seeing as any small change in initial conditions could completely change the resulting pattern. Many scientists today have theories and models of chaotic global climate systems, but it will take many years of study to determine a model that can even remotely mimic the patterns we see today.

In the effort to improve these models, we study climate patterns. Some of the patterns, known as teleconnections, affect weather patterns both locally and at a distance. They can span days, weeks, months, or even centuries. They are a significant aspect in the chaos of our dynamic atmospheric system. Some of the longest lasting patterns we have names for and are still being studied, like El Niño Southern Oscillation (ENSO), the main pattern we will be studying in this paper.

ENSO is one of the most important climate phenomena on earth due to its global influence on other weather patterns. ENSO has a direct impact on the rainfall patterns in the tropics and has a strong effect on the US national weather as well as other parts of the world. It gets a lot of attention because it is somewhat predictable, often precursors are seen before its effects make an impact.

Historically, ENSO was first noticed by an English physicist and statistician Sir Gilbert Walker. He studied applied mathematics in a variety of fields; aerodynamics, electromagnetism and the analysis of time-series data. He was not a meteorologist, but was hired for a statistician position in a Meteorology Department in India. He had much success here, coming up with a method for studying weather parameters that was later named after him and George Udny Yule called the Yule-Walker Equations [8]. In 1928, he published a paper observing the "Southern Oscillation" of atmospheric pressure between the Indian Ocean and the Pacific, which later was named El Niño Southern Oscillation [24]. His contributions were significant to the future of meteorology. They named the convection cell the Walker Circulation after him.

The Walker Circulation is a convection cell that runs east to west across the tropical pacific. As you can see in the Figure 1, the convection cell is affected by the phase of ENSO due to the changing sea surface temperatures (SST).

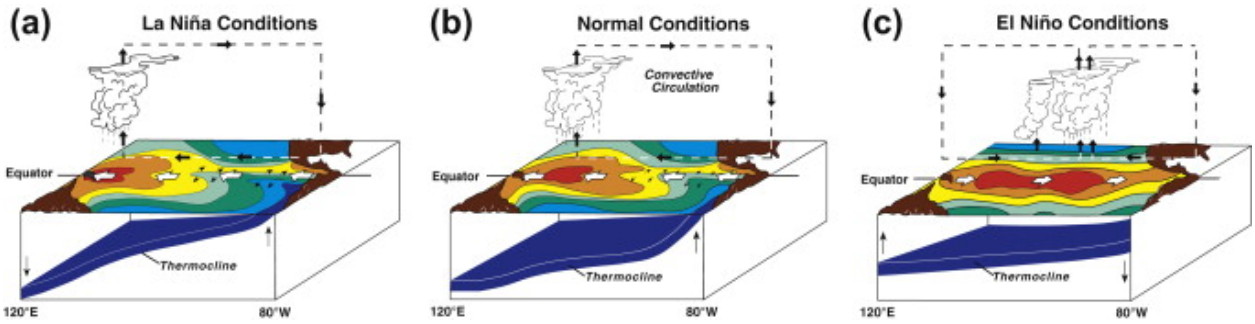

Figure 1: **Walker Circulation Cell** a) During La Niña the easterly wind strengthens, upwelling of cold water increases in the east, and precipitation increases in the west. b) Under normal conditions there is upwelling in the eastern pacific due to average strength easterly winds. c) During El Niño conditions the easterly winds weaken, upwelling halts in the east,and precipitation is moved further east.

The Hadley Circulation is the convection of air that rises at the Inter-Tropical Convergence Zone, or ITCZ, and sinks at 30°N and 30°S. The ITCZ is a belt of low pressure which circles the Earth generally near the equator where the trade winds of the Northern and Southern Hemispheres come together [20].

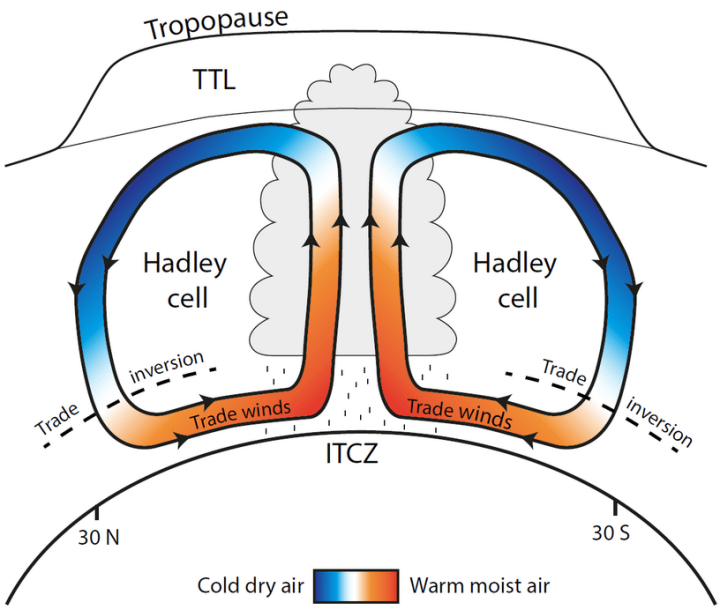

Figure 2: Hadley Circulation Cell: Under normal conditions the ITCZ will be near the equator. During El Niño conditions SSTs in the Central Pacific warm, and the Hadley cell is strengthened by the warmer water at the equator. Causing changes in precipitation patterns around the globe, one of ENSO's teleconnections if you will.

El Niño is a climate pattern characterized by unusually warm surface waters of the

central and eastern Equatorial Pacific. Conversely, La Niña is characterized by unusually cold surface temperatures. The variance from "normal" temperatures of only about 1-3 degrees influences the tropical Pacific Ocean Atmospheric System, which in turn impacts weather and climate around the world. This variance oscillates from normal to El Niño or La Niña every three to seven years and is referred to as the ENSO climate cycle[14]. When the conditions are "normal" it is referred to as ENSO neutral, and is usually only the time period between ENSO phases. El Niño has typical effects on global climate. Indonesia has decreased rainfall while the tropical Pacific Ocean has increased rainfall. The normally prevailing easterly winds which normally blow from east to west along the equator die down, and sometimes even reverse direction. The more the surface temperatures warm the more these effects strengthen.

La Niña's typical characteristics are reverse of El Niño patterns. Thus the cooling of the Pacific Ocean surface temperatures results in Indonesia rainfall increasing and Pacific rainfall decreasing, and a strengthening of the easterly winds across the equator from east to west.

During the Neutral phase of ENSO temperatures remain somewhat close to average. In some years there may be a variance in ocean surface temperatures but without the characteristic effects following.

The Oscillation between ENSO phases depends on underlying tropical Pacific thermocline. A thermocline is a boundary of rapidly changing temperature. For the Pacific, this refers to the separation of relatively warm and cold sea water.

What causes the shift in SSTs during Neutral and La Niña conditions? As seen in Figure 3, during Neutral conditions the thermocline slopes towards the west. Thus allowing the upwelling of denser cold water to the surface of the Eastern Pacific off the coast of Peru. During La Niña, this shift is exaggerated, allowing for stronger upwelling of cold water, and a decrease in temperatures at the surface, the temperatures of which can be seen by satellites.

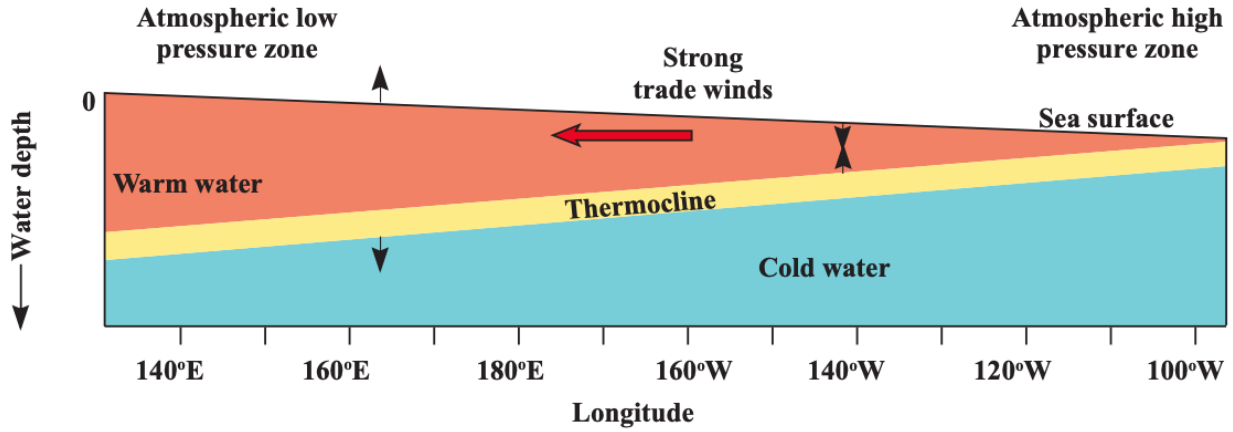

Figure 3: The left side of the figure represents the Western Pacific Ocean, and the right side of the figure represents the Eastern Pacific.

Now, what happens during El Niño conditions? During an El Niño event the thermocline slopes east as a result of the weakening of the Easterly Tradewinds. This prevents the denser

cold water under the thermocline from upwelling to the surface. The SSTs of the Eastern Pacific increase as the normal upwelling of cold water is obstructed. This temperature increase can also be seen by satellites.

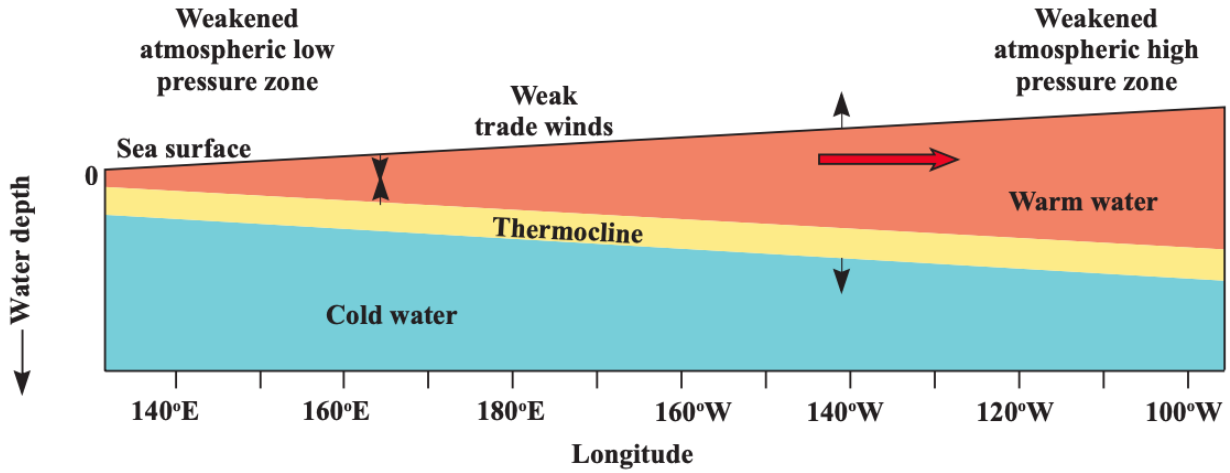

Figure 4: The directions are the same as in Figure 3, except that the thermocline is now sloping in the opposite direction due to the shift in the wind direction.

Normally prevailing westward winds due to the Coriolis effect create a zone of upwelling off the coast of Peru. The upwelling of cold water brings up high concentrations of nutrients from the depths of the ocean that are essential to phytoplankton growth. Thus, these upwelling zones have high primary productivity rates, and schools of anchovy feed on the abundant phytoplankton blooms that grow in the Peruvian upwelling region. The anchovy populations here were once so large that they yielded about 20% of the world's total fish catch, that is until they were overfished[17].

However, when the Eastern Pacific Ocean surface waters warm during El Niño the normally cold water gets displaced by the less dense warm water and causes a stable stratification of the water column and inhibits upwelling. This dramatically reduces the amount of nutrients near the coast and thus spurs a decimation of the thriving fishery which can be an early indicator of a shift of ENSO phases[17].

A way that ENSO is monitored is through the use of 4 oceanic indices. Each index refers to a region of the tropical Pacific Ocean where SST's are averaged and monitored.

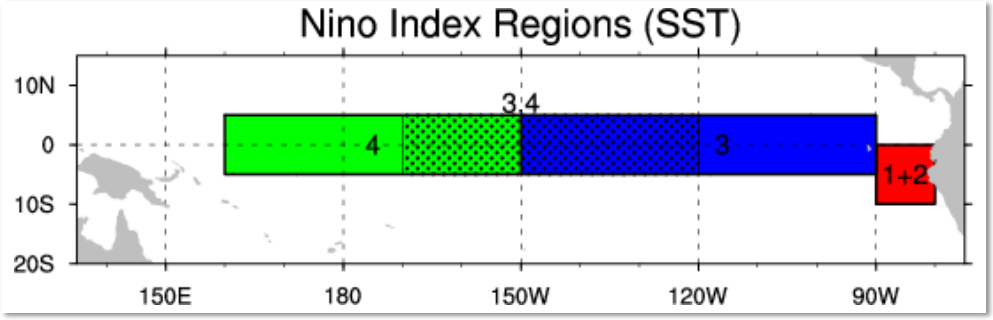

Figure 5: Tropical Pacific Niño Index Regions

Anomalies in these Index regions are early indicators of an ENSO event. The Niño 3.4 is the most commonly used region to define an El Niño or La Niña event by NOAA. The global effects of ENSO events respond to the severity of variation of these SST's from average.

The Southern Oscillation Index, or SOI, is a measure of the large-scale fluctuations in air pressure occurring between the western and eastern tropical Pacific (i.e., the state of the Southern Oscillation) during El Niño and La Niña episodes. It another way to predict ENSO events in the tropical Pacific Ocean.

With respect to weather in the Andes Mountains, the westerly wind anomalies that occur during El Niño block moist Amazonian air from reaching the leeward (western) side of the Cordillera Blanca causing reduced precipitation, warmer temperatures, and increased glacial melt. The strong easterly winds associated with La Niña tend to push the moist air over the range supporting increased precipitation, cooler temperatures, and snow accumulation that increases the size of glaciers.

1.2 Introduction to Peru, its Glaciers, Climate and Community Needs

The tropical Andes is facing critical water resource issues as mountain valleys experience persistent glacier recession [23]. This project focuses on Peru's Rio Santa Valley and the region surrounding the Cordillera Blanca (CB) or White Mountains (Figure 5), which is Earth's most glacierized tropical mountain range. Glacial-fed tributaries flow from pro-glacial valleys carved out by receding glaciers in the CB to supply about two thirds of discharge to the upper Santa River [11], whose waters are utilized for municipal supplies, hydroelectric generation, and agricultural irrigation to the Pacific coast [10] [4].

Recent satellite image analysis has indicated accelerated recession of CB glaciers and a 25 percent loss of their area between 1987 and 2010 [3][15][18]. The well documented, persistent decline of the glaciers in the Cordillera Blanca will likely put strain on water resources in the near future for populations living adjacent to the range in the Rio Santa Valley as fresh water sourced from glacial melt becomes increasingly limited [18][1] [10]. Glaciers are sensitive indicators of climate change as their surface energy balance is related to the temperature and precipitation in the overlying atmosphere [12]. The rapid loss of glacierized area in the CB has increased the need for greater understanding of the factors controlling the elevation of the freezing level during precipitation events, which has been shown to be crucial for the ablation process [2].

Where is the Rio Santa Basin?

Figure 6

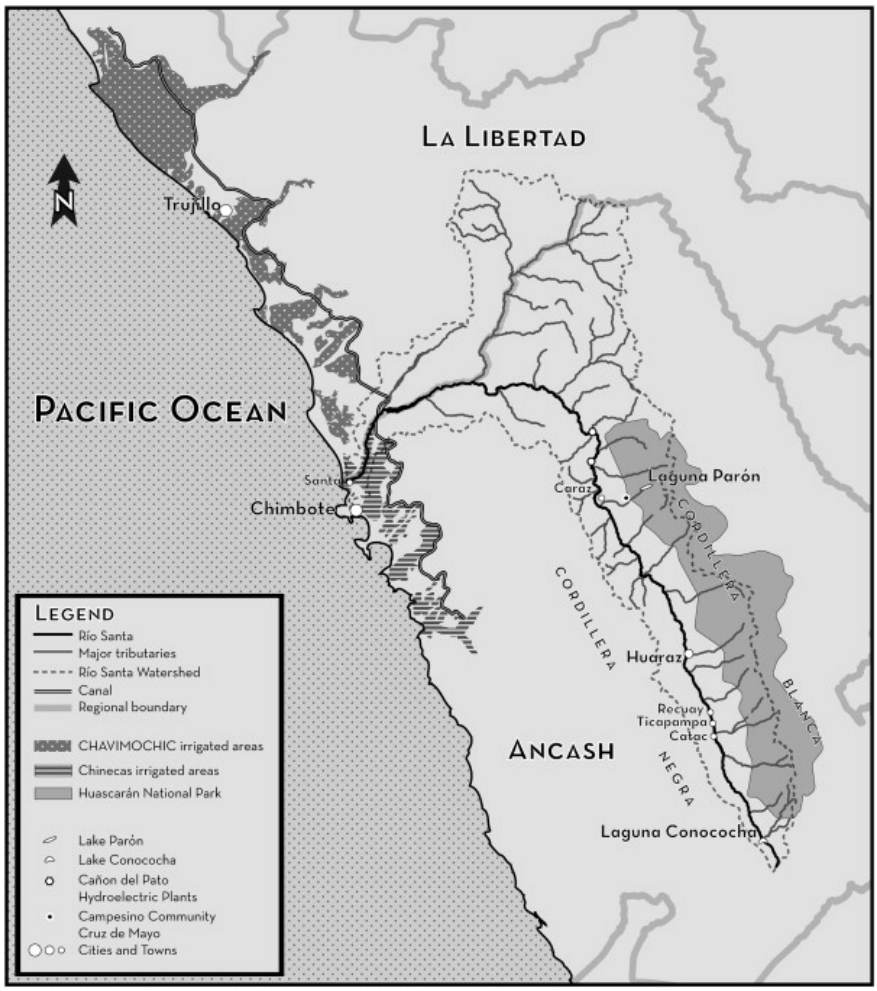

Figure 7

The climate in the CB is semi-arid in the valleys and moist in higher elevations with a distinct rainy season between October and April and dry the remaining months [7]. Changes in ocean temperature off the coast of Peru and extending into the central Pacific impact the glacier mass balance and therefore the dry season (May-September) water supply, which is critical for drinking water, crop irrigation and hydroelectic energy production. Furthermore, ENSO events modulate the intensity of rainfall and air temperature and this creates hazards such as glacial lake outburst floods (GLOFs) caused by glacier and rock debris avalanches falling into melt-water lakes with enough momentum to break through dams or natural rock formations. In the past few decades, the increasingly warming climate has caused the volume of the glacial lakes in Cordillera Blanca to expand rapidly. The potential energy of the water converts to kinetic energy sending torrents of water dropping up to over 1000 meters from mountain sides to devastate communities in their wake [13].

2 Methods

There were two sources for the data. Satallite based SST data, and SOI data was used to represent the ENSO phases. The data was collected from the NOAA data archives, where the agency is studying the dynamics of the Niño Index regions[21].

The weather station data were acquired with permission from Dr. Mario Rohrer (personal communication), Managing Director of Meteodat.ch in Zurich Switzerland, who has expertise in energy and meteorology. The password protected data portal was created under the Glaciers Project which was a grant-supported collaboration between Swiss and Peruvian meteorologists (and hydrologists) from the National Service of Meteorology and Hydrology of Peru (SENAMHI). Data are available at six-hourly and daily resolution including: max/min air temperature and humidity and total precipitation [19].

A 30-year time range was chosen for this project, which is typical for a climate study. The time range from 1990-2019 is long enough to see several seesaws between La Niña and El Niño phases, which are characterized by changing SSTs. It is expected that there will be some correlation between the sea surface temperatures changes and the ground based weather station measurements of temperature and precipitation.

To determine the strength of the relationships, the SST and weather data were graphed with a superimposed linear regression. The R-square, or the coefficient of determination, values for each station were placed into a table and graphed, clarifying which relationships are strongest and for identifying outliers.

For example, the coefficient of determination could be thought of as a percentage of how many data points fall on the line formed by the linear regression. The higher the coefficient, the higher percentage of points the line passes through when the data points and line are plotted. If the coefficient is 0.80, then 80% of the points should fall on the regression line. Values of 1 or 0 would indicate the regression line represents all or none of the data, respectively. A higher coefficient is an indicator of a better goodness of fit for the observations and in comparing meteorological variables that are thousands of meters apart and at different elevations with many, uncontrollable, indeterminable and unknown factors influencing the response, typical coefficients expecting between nearly zero and about 0.7 [5].

$$R^2 = \left(\frac{n(\sum xy) - (\sum x)(\sum y)}{\sqrt{\left[n\sum x^2 - (\sum x)^2\right]\left[n\sum y^2 - (\sum y)^2\right]}} \right)^2 \tag{1}$$

2.1 Ground Based Data

First, the stations had to be selected. There are several weather stations throughout the White Mountains of Peru, they are displayed in Figure 8 as yellow pins.

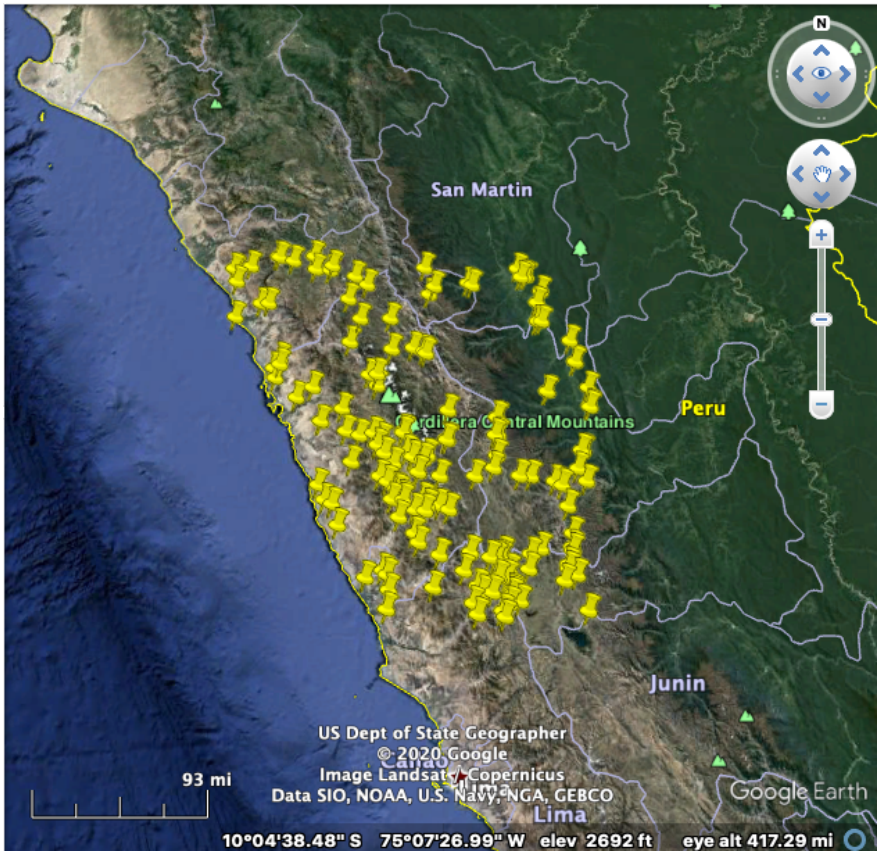

Figure 8: There are dozens of weather stations to look at throughout the White Mountains.

Although there are many stations available, it can be tricky determining which stations are useful. For this project the stations selected had to have data within the chosen time range of 1990 to 2019. Some of the stations had data that goes all the way back to the 19 century, but a select few recorded all the way up to present day. In the end the weather stations with useable data were Alto Peru, Mollepata 1, Chavin 1, Oyon, and Lake Cochaquillo (also referred to as Laguna Cochaquillo).

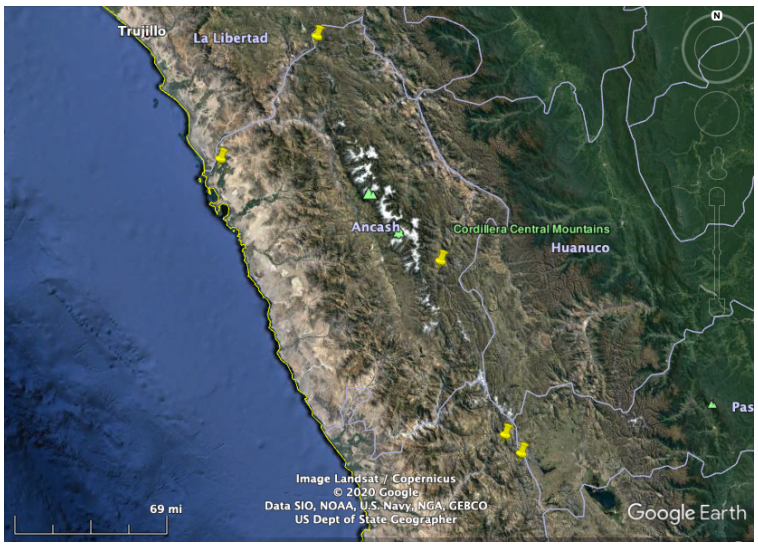

Figure 9: From the stations available only 5 were chosen for this project, shown as yellow pins.

These stations had a variety of data available, and all that was needed was the temperature and precipitation measurements. Early on in this process it was uncertain if the humidity measurements would be needed, so those were included for the data synthesis.

The weather station data was pulled from the Meteodat portal [19] and converted from a text file to excel. From here separate tables were created for each weather station location.

The data was quality checked and organized so each row was time in days, and each column was a different kind of weather variable; temperature maximum and minimum measurements for that day; humidity measurements at 0700, 1300, 1900 hours that day; precipitation total.

Temperature and humidity measurements were combined into one averaged daily measurement. Then the measurements were averaged for every 30 days, to become an approximate monthly average. Daily precipitation was totaled for each of these 30 day sets. This condensed the data into one table for each weather station.

Month	Year Fraction
January	1990.00
February	1990.08
March	1990.17
April	1990.25
May	1990.33
June	1990.42
July	1990.50
August	1990.58
September	1990.67
October	1990.75
November	1990.83
December	1990.92

Figure 10: Example 3.1: Decimal system representation of months.

Having a common time-stamp and format is critical for synchronization for comparison and analysis. The monthly time was converted into a decimal system in years for a better time representation. In Example 3.1, the month was converted to a decimal by dividing the number of the month by the total months (12).

The next step after this was to determine the phase of El Niño for each month. This was done by using looking at the United States National Oceanic and Atmospheric Administration's (NOAA) Multivariate ENSO Index (MEI) data.

The MEI.v2 uses observations from NOAA Climate Data Record (CDR) of Monthly Outgoing Longwave Radiation (OLR) [14]. to create a normalized 40 year average. Shown below are the tables of MEI data for each decade. They are in 3 month averages with color coding for each phase. Blue text means that month was greater than -0.5 standard deviations away from average. Black text means that month was within +/-0.5 standard deviations of the average. Red means that month was greater than +0.5 standard deviations away from average.

Year	DJF	JFM	FMA	MAM	AMJ	MJJ	JJA	JAS	ASO	SON	OND	NDJ
1990	0.1	0.2	0.3	0.3	0.3	0.3	0.3	0.4	0.4	0.3	0.4	0.4
1991	0.4	0.3	0.2	0.3	0.5	0.6	0.7	0.6	0.6	0.8	1.2	1.5
1992	1.7	1.6	1.5	1.3	1.1	0.7	0.4	0.1	-0.1	-0.2	-0.3	-0.1
1993	0.1	0.3	0.5	0.7	0.7	0.6	0.3	0.3	0.2	0.1	0.0	0.1
1994	0.1	0.1	0.2	0.3	0.4	0.4	0.4	0.4	0.6	0.7	1.0	1.1
1995	1.0	0.7	0.5	0.3	0.1	0.0	-0.2	-0.5	-0.8	-1.0	-1.0	-1.0
1996	-0.9	-0.8	-0.6	-0.4	-0.3	-0.3	-0.3	-0.3	-0.4	-0.4	-0.4	-0.5
1997	-0.5	-0.4	-0.1	0.3	0.8	1.2	1.6	1.9	2.1	2.3	2.4	2.4
1998	2.2	1.9	1.4	1.0	0.5	-0.1	-0.8	-1.1	-1.3	-1.4	-1.5	-1.6
1999	-1.5	-1.3	-1.1	-1.0	-1.0	-1.0	-1.1	-1.1	-1.2	-1.3	-1.5	-1.7

Figure 11: MEI data 1990's

Year	DJF	JFM	FMA	MAM	AMJ	MJJ	JJA	JAS	ASO	SON	OND	NDJ
2000	-1.7	-1.4	-1.1	-0.8	-0.7	-0.6	-0.6	-0.5	-0.5	-0.6	-0.7	-0.7
2001	-0.7	-0.5	-0.4	-0.3	-0.3	-0.1	-0.1	-0.1	-0.2	-0.3	-0.3	-0.3
2002	-0.1	0.0	0.1	0.2	0.4	0.7	0.8	0.9	1.0	1.2	1.3	1.1
2003	0.9	0.6	0.4	0.0	-0.3	-0.2	0.1	0.2	0.3	0.3	0.4	0.4
2004	0.4	0.3	0.2	0.2	0.2	0.3	0.5	0.6	0.7	0.7	0.7	0.7
2005	0.6	0.6	0.4	0.4	0.3	0.1	-0.1	-0.1	-0.1	-0.3	-0.6	-0.8
2006	-0.8	-0.7	-0.5	-0.3	0.0	0.0	0.1	0.3	0.5	0.7	0.9	0.9
2007	0.7	0.3	0.0	-0.2	-0.3	-0.4	-0.5	-0.8	-1.1	-1.4	-1.5	-1.6
2008	-1.6	-1.4	-1.2	-0.9	-0.8	-0.5	-0.4	-0.3	-0.3	-0.4	-0.6	-0.7
2009	-0.8	-0.7	-0.5	-0.2	0.1	0.4	0.5	0.5	0.7	1.0	1.3	1.6

Figure 12: MEI data 2000's

Year	DJF	JFM	FMA	MAM	AMJ	MJJ	JJA	JAS	ASO	SON	OND	NDJ
2010	1.5	1.3	0.9	0.4	-0.1	-0.6	-1.0	-1.4	-1.6	-1.7	-1.7	-1.6
2011	-1.4	-1.1	-0.8	-0.6	-0.5	-0.4	-0.5	-0.7	-0.9	-1.1	-1.1	-1.0
2012	-0.8	-0.6	-0.5	-0.4	-0.2	0.1	0.3	0.3	0.3	0.2	0.0	-0.2
2013	-0.4	-0.3	-0.2	-0.2	-0.3	-0.3	-0.4	-0.4	-0.3	-0.2	-0.2	-0.3
2014	-0.4	-0.4	-0.2	0.1	0.3	0.2	0.1	0.0	0.2	0.4	0.6	0.7
2015	0.6	0.6	0.6	0.8	1.0	1.2	1.5	1.8	2.1	2.4	2.5	2.6
2016	2.5	2.2	1.7	1.0	0.5	0.0	-0.3	-0.6	-0.7	-0.7	-0.7	-0.6
2017	-0.3	-0.1	0.1	0.3	0.4	0.4	0.2	-0.1	-0.4	-0.7	-0.9	-1.0
2018	-0.9	-0.8	-0.6	-0.4	-0.1	0.1	0.1	0.2	0.4	0.7	0.9	0.8
2019	0.8	0.8	0.8	0.7	0.6	0.5	0.3	0.1	0.1	0.3	0.5	0.5

Figure 13: MEI data 2010's

This color coding from the MEI data was brought over for use in the tables marking each month to categorize it by ENSO phase.

The color coding was especially helpful for sorting the data by phase. All existing data up to that point was in a large table of all the monthly averaged data. This table was then sorted by phase and then separated into 3 tables; One for El Niño phase, one for Neutral phase and one for La Niña phase. These tables still contained the temperature, humidity and precipitation measurements.

2.2 SST Data

Then the next step was to add SST values from the NOAA archives [21]. The SSTs were added for each Niño Index to the each site's table. The data had already been synthesized by NOAA. The data just had to be chronologically included with the ground based measurements.

These tables were graphed with a superimposed line of best fit, all of which are shown in Appendix 7.1. The line of best fit came from the linear regression.

A graph of the NOAA SST data has been included to show the time series representation of each separate Niño Index.

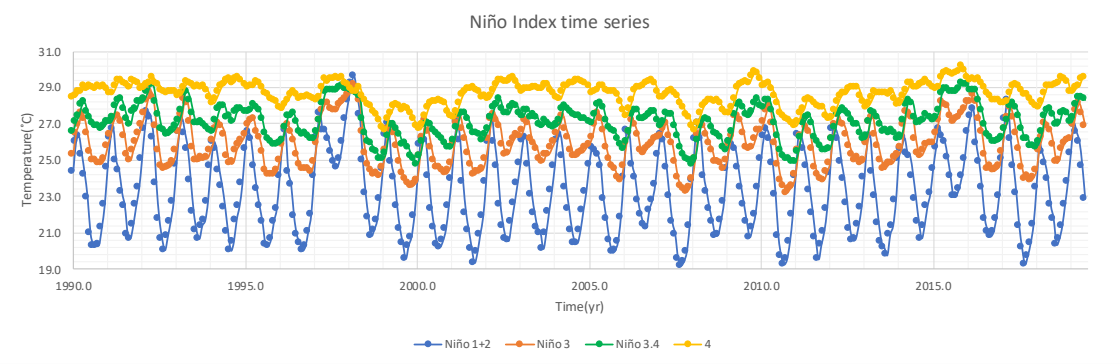

Figure 14: SSTs from Satellite Observations

It is apparent from the Figure 14, that the Niño 1+2 temperature range is the largest. There is are two distinct abnormalities that stand out: the warm events from 1997-1998 and again in 2015-2016.

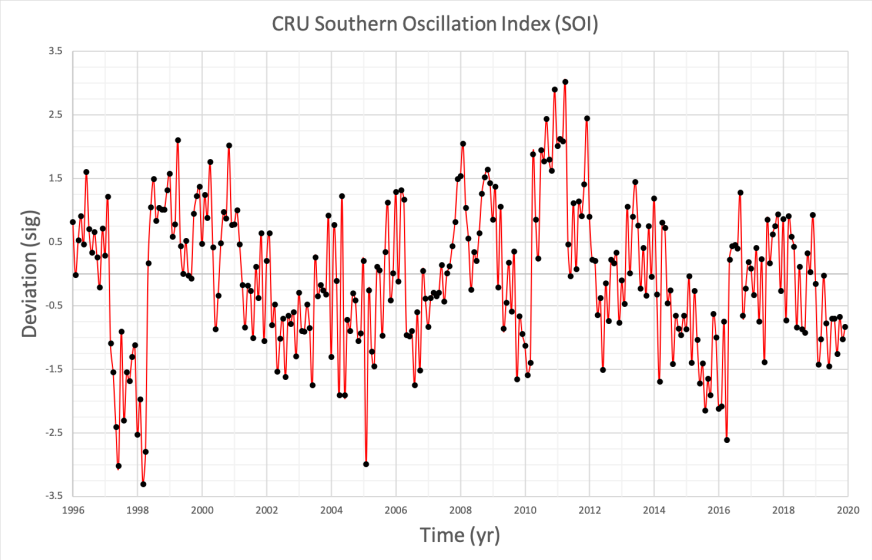

Figure 15

The above figure is the SOI data in a time domain graph. It shows that in 1998 and again in 2012 there are significant deviations from average.

3 Results

After the data was synthesized in a table it was graphed with SSTs as well as the linear regression. All these individual graphs can be viewed in Appendix 7.1 under Tables and Graphs. From these graphs the linear regressions gave an R-Square value. These R-Square values were graphed vs elevation in the Figures 16-20 for comparison.

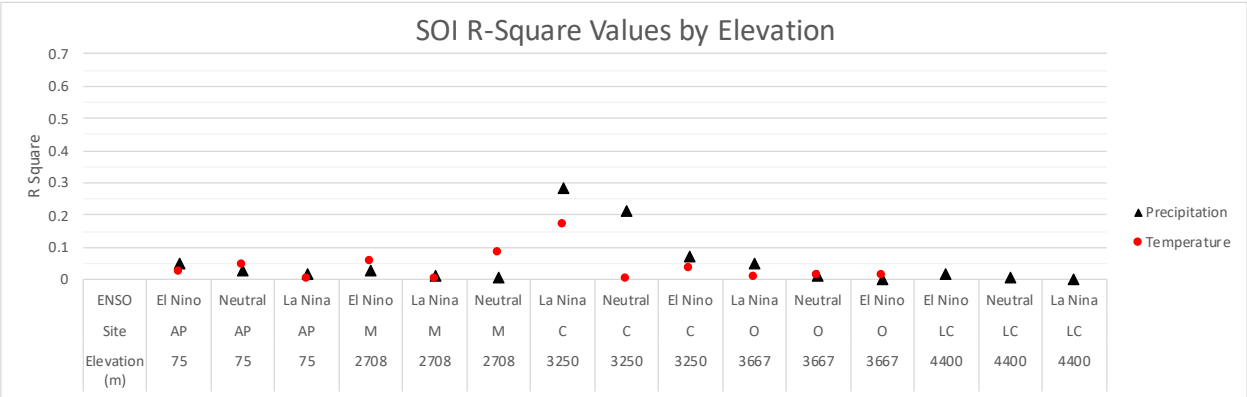

Figure 16: SOI R-Square Values: Red dots represent Temperature, and black triangles represent Precipitation.

For the SOI, the site of Chavin (3250 m) has the largest R-Square value at 30% correlation. The La Niña and Neutral phases of ENSO have stronger relationships with the ground based data than the El Niño phase. At Chavin, the Precipitation seems to have a higher R-Square value than its corresponding Temperature R-Square value. The rest of the sites have less than 10% correlation.

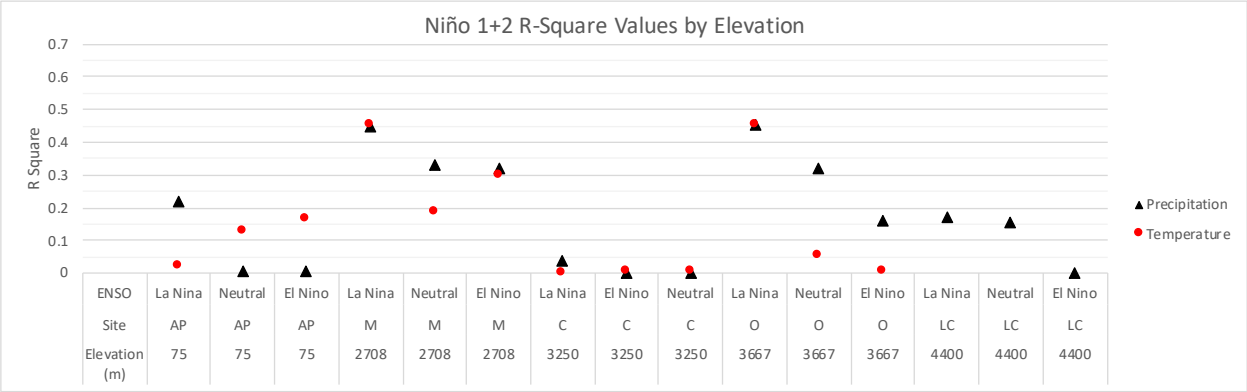

Figure 17: Niño 1+2 Index R-Square Values: The highest R-Square values seem to be the La Niña Phase.

In the comparison of R-Square with the Niño 1+2 Index, the highest notable values are both at 46%, for the La Niña phase of Mollepata and Oyon, which are at 2708m and 3667m respectively. Overall for this Index, the La Niña phase seems to have a stronger correlation. As for ground based data, the precipitation is higher correlated than air temperature, with the exception of Alto Peru during La Niña. Lake Cochaquillo does not possess air temperature data, that is why there is no red dots on the graphs for this location.

Alto Peru has a R-Square value range of 0-22%. Molletpata has a R-Square value range of 19-46%. Chavin has a R-Square value range of less than 5%. Oyon has R-Square value range of 0-47%. Laguna Cochaquillo has a R-Square value range of 0-17%.

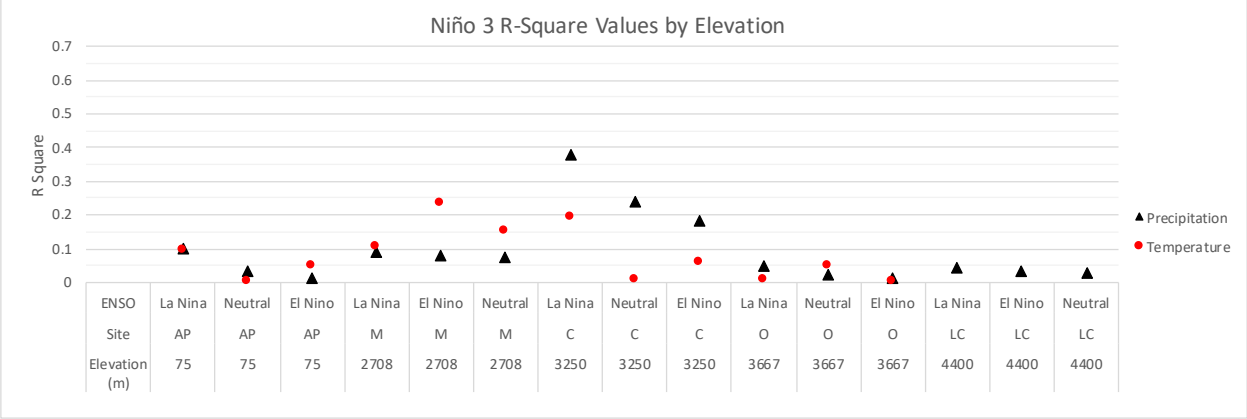

Figure 18: Niño 3 Index R-Square Values: The highest R-Square values seem to be the La Niña Phase.

In the comparison of R-Square with the Niño 3 Index, the highest notable value is at

38%, for the precipitation of the La Niña phase of Chavin, which is at 3250m. Mollepata had a stronger relationship with precipitation than air temperature, unlike the other sites.

Alto Peru has a R-Square value range of 0-11%. Molletpata has a R-Square value range of 7-24%. Chavin has a R-Square value range of less than 0-37%. Oyon has R-Square value range of 0-6%. Laguna Cochaquillo has a R-Square value range of 2-4%.

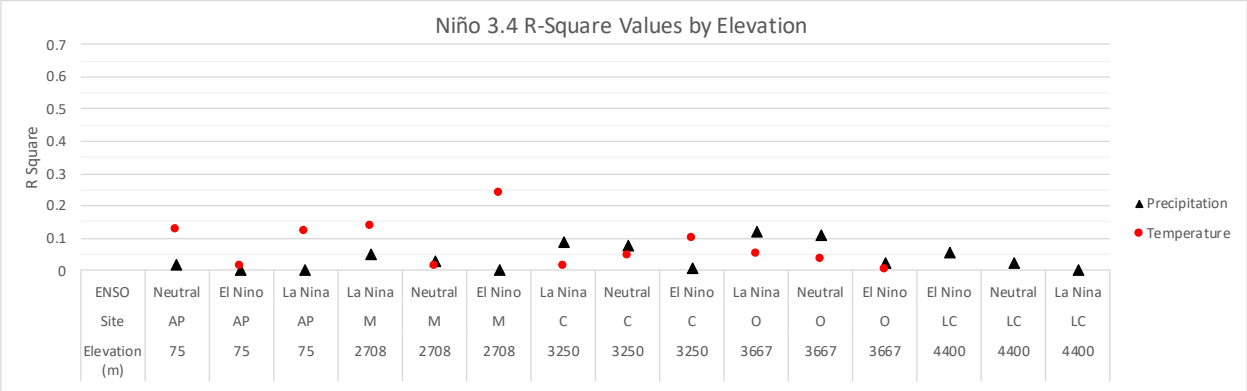

Figure 19: Niño 3.4 Index R-Square Values: The highest R-Square values seem to be the El Niño Phase.

In the comparison of R-Square with the Niño 3.4 Index, the highest notable value is at 24%, for the air temperature of the El Niño phase of Mollepata, which is at 2708m. Air temperature has a stronger correlation at lower elevation, but precipitation has a stronger correlation at higher altitudes.

Alto Peru has a R-Square value range of 0-14%. Molletpata has a R-Square value range of 0-24%. Chavin has a R-Square value range of less than 0-11%. Oyon has R-Square value range of 0-6%. Laguna Cochaquillo has a R-Square value range of 2-4%.

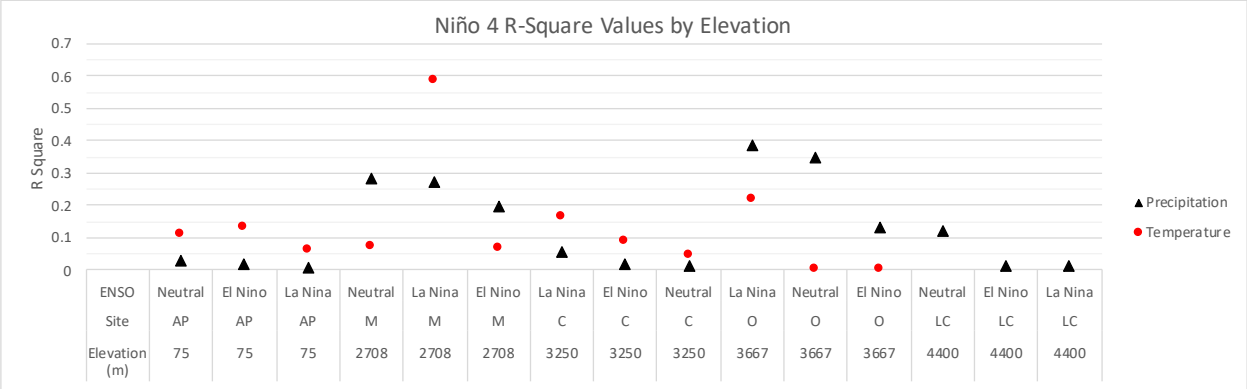

Figure 20: Niño 4 Index R-Square Values: The highest R-Square values seem to be the La Niña Phase.

In the comparison of R-Square with the Niño 4 Index, the highest notable temperature value is at 58% correlation, for the La Niña phase of Mollepata, which is at 2708m. The highest notable precipitation values is at 35-38% correlation for both the La Nina and the

Neutral phase of Oyon, at 3667m. Again we see that air temperature has a stronger correlation at lower elevation, but precipitation has a stronger correlation at higher altitudes. Overall, the La Niña and Neutral phases have stronger correlations than the El Niño phase.

Alto Peru has a R-Square value range of 0-14%. Molletpata has a R-Square value range of 7-58%. Chavin has a R-Square value range of less than 0-19%. Oyon has R-Square value range of 0-38%. Laguna Cochaquillo has a R-Square value range of 0-12%.

4 Discussion and Conclusions

The results provide several interesting outcomes that shed light on the connection between ENSO and the weather patterns in the mountains. The lower elevations had a higher air temperature R-square value with the SSTs. The higher elevations had a higher precipitation R-square value with the SSTs. Furthermore, four out of the five Niño Index R-Square graphs had the strongest ENSO phase correlation with La Niña. It is important to notice that the graphs for Niño 1+2 and Niño 4 had high two peaks in R-square that correspond to elevations of 2708 m and 3667 m with very low R-square between these two elevations. This suggests that there is a strong influence of the mountain ridge between these two elevations. Another point to make is that Niño 3.4 has the lowest R-Square values out of the all the SST Indices which is interesting considering that NOAA depends more heavily on this Index for determining ENSO phases. Up at high elevations in the White Mountains, Lake Cochaquillo data seemed to be unaffected by the ENSO phases except for the Niño 1+2 where it was almost a 20% correlation for both La Niña and Neutral phases. This indicates that the high elevations may only be affected by the closest Niño Index region.The data show that a majority of the comparisons display a stronger relationship between La Niña phase SSTs and the ground based measurements than the Neutral and the El Niño phases of ENSO.

4.1 Uncertainties in Data

The data was averaged at every 30 days, with the knowledge that months vary from 28 to 31 days. But if you take an average of these months, you will find the average to be 30.44 days. This was simply rounded down to 30 days per month, with the assumption that the data would still be present even if the 1 or 2 days are in the misrepresented month.

The temperature measurements have an uncertainty of about $\pm$0.5C. As for the precipitation measurements, they have a higher uncertainty due to the science of measuring precipitation. This is due to wind and under catch, but all stations have this effect to their measurements, it can vary $\pm$20%.

The humidity data was averaged, but it was not used to graph because it was determined that another study would be needed with the dewpoint in order to determine the significance of the relationship.

Many locations had inconsistant time series data. Chavin had data from 1990-2019, with one month missing in April 2004. Mollepata had precip data from 1996-2019, but only temperature data from 2015-2019. Oyon had both precipitation and temperature data from 1996-2019. Alto Peru has precipitation and temperature data 2000-2006. Laguna Cochaquillo has only precipitation from 1995-2019.

If I was to attempt to do a similar study again, I would find a time range that would be better represented by the ground based measurements. That means finding more stations, stations with complete 30 year time ranges, and stations with data for precipitation, temperature, humidity, and dewpoint.

There were several interesting patterns found that may be impactful to our knowledge of these glacierized White Mountains. But there is potential for more work in the future.

5 Proposed Future Work

There seems to be a worthy discussion needed about what causes the El Niño events (is it the chicken or the egg). Does the shifting of the pressure systems cause the winds that cause the change in the SST? Or the more likely, that the amount of solor radiation that the surface of the ocean absorbs, heats the air above it causing the air pressure to decrease above it, which causes the air pressure systems to change which causes the winds to shift, resulting in the physical shifting of the thermocline.

A project for the future could be analyzing the freqency in oscillations of the ENSO events from the last 100 years to the past two decades. It is apparent that the oscillations are becoming more frequent.

Another project would be to look into how humidity and dewpoint are correlated with this data series.

References

[1] Baraer, M., B. G. Mark, J. M. Mckenzie, T. Condom, J. Bury, K. Huh, and others (2012), Glacier recession and water resources in Peru's Cordillera Blanca, *Journal of Glaciology* 58: 134-150. doi: 10.3189/2012JoG11J186.

[2] Bradley, R. S., F. T. Keimig, H. F. Diaz, and D. R. Hardy. 2009. Recent changes in freezing level heights in the Tropics with implications for the deglacierization of high mountain regions. *Geophysical Research Letters* 36: L17701.

[3] Burns, P. and A. Nolin. 2014. Using atmospherically-corrected Landsat imagery to measure glacier area change in the Cordillera Blanca, Peru from 1987 to 2010. *Remote Sensing of Environment* 140: 165-178.

[4] Bury, J., B. G. Mark, M. Carey, K. R. Young, J. M. McKenzie, M. Baraer, A. French, and M. H. Polk. 2013. New Geographies of Water and Climate Change in Peru: Coupled Natural and Social Transformations in the Santa River Watershed. *Annals of the Association of American Geographers* 103: 363-374.

[5] *Coefficient of Determination (R Squared): Definition, Calculation*, (Statistics How To, 2019).

[6] Fiehn, Alina, *Transport of very short-lived substances from the Indian Ocean to the stratosphere through the Asian monsoon.* (Fiehn 2010)

[7] Kaser, G. and H. A. Osmaston. 2002. Tropical Glaciers. Cambridge: Cambridge University Press.

[8] Katz, Richard W., *Sir Gilbert Walker and a Connection between El Niño and Statistics.*, (Statistical Science, Institute of Mathematical Statistics, 1986).

[9] L'Heureux, Michelle., *Oceanic Kelvin Waves: The next Polar Vortex*: NOAA Climate.gov.*, (NOAA Climate.gov, 2015).

[10] Mark, B. G., J. Bury, J. M. McKenzie, A. French, and M. Baraer. 2010. Climate Change and Tropical Andean Glacier Recession: Evaluating Hydrologic Changes and Livelihood Vulnerability in the Cordillera Blanca, Peru. *Annals of the Association of American Geographers* 100: 794-805.

[11] Mark, B. G., J. M. McKenzie, and J. Gomez. 2005. Hydrochemical evaluation of changing glacier meltwater contribution to stream discharge: Callejon de Huaylas, Peru. *Hydrological Sciences Journal-Journal Des Sciences Hydrologiques* 50: 975-987.

[12] Oerlemans, J., and E. J. Klok. 2002. Energy balance of a glacier surface: analysis of automatic weather station data from the Morteratschgletscher, Switzerland. *Arctic, Antarctic, and Alpine Research* 34(4): 477. doi:10.2307/1552206.

[13] Palmer, J. 2019. The dangers of glacial lake floods: Pioneering and capitulation, *Eos*, 100. https://doi.org/10.1029/2019EO116807.

[14] Psl., *Multivariate ENSO Index Version 2 (MEI.v2)*, (PSL, 2020).

[15] Rabatel, A., B. Francou, A. Soruco, J. Gomez, B. Cáceres, J. L. Ceballos, R. Basantes, M. Vuille, J. E. Sicart, C. Huggel, M. Scheel, Y. Lejeune, Y. Arnaud, M. Collet, T. Condom, G. Consoli, V. Favier, V. Jomelli, R. Galarraga, P. Ginot, L. Maisincho, J. Mendoza, M. Ménégoz, E. Ramirez, P. Ribstein, W. Suarez, M. Villacis, and P. Wagnon. 2013. Current state of glaciers in the tropical Andes: a multicentury perspective on glacier evolution and climate change. *Cryosphere* 7: 81–102.

[16] Sarachik, Edward S.and Cane, Mark A., *The El Nino-Southern Oscillation Phenomenon*, (Pearson/Addison Wesley, 2017) Ch. 1-2, pp. 1–60.

[17] Segar, Douglas A. , *Ocean and Atmosphere Interactions*, (Reefimages, 2018) Ch.7.

[18] Schauwecker, S., M. Rohrer, D. Acuña, A. Cochachin, L. Dávila, H. Frey, C. Giráldez, J. Gómez, C. Huggel, M. Jacques-Coper, E. Loarte, N. Salzmann, and M. Vuille. 2014. Climate trends and glacier retreat in the Cordillera Blanca, Peru, Revisited. *Global and Planetary Change* 119: 85-97.

[19] Schwarb, M., Acuña, D., Konzelmann, T., Rohrer, M., Salzmann, N., Serpa Lopez, B., Silvestre, E.,2011. A data portal for regional climatic trend analysis in a Peruvian High Andes region.Advances in Science and Research 6, 219–226.

[20] SKYbrary Wiki., *Inter Tropical Convergence Zone (ITCZ) - SKYbrary Aviation Safety*, (SKYbrary Aviation Safety, 2018).

[21] Smith, Cathy, *Analyze Plot Long Range Climate Timeseries*, (NOAA Physical Sciences Laboratory, 2016).

[22] Talley, Lynne D., *Descriptive Physical Oceanography (Sixth Edition)*, (Academic Press, 2012).

[23] Vuille, M., B. Francou, P. Wagnon, I. Juen, G. Kaser, B. G. Mark, and R. S. Bradley. 2008. Climate change and tropical Andean glaciers: Past, present and future. *Earth-Science Reviews* 89: 79-96.

[24] Walker, Gilbert., *Royal Meteorological Society Journals*, (John Wiley Sons, 2007).

[25] Water.org, *Peru's Water Crisis - Water In Peru 2019*, (Water.org, 2020).

6 Appendix

6.1 Weblinks

Meteodat
SENAMHI
NOAA Plots
NOAA Past Events
MEI Data
Walker and El Niño
Segar, Ocean Sciences
Gilbert Walker Paper
Kelvin Wave
Water.org
Descriptive Physical Oceanography
Hadley Circulation Figure
ITCZ
Coefficient of Determination

6.2 Graphs and Tables

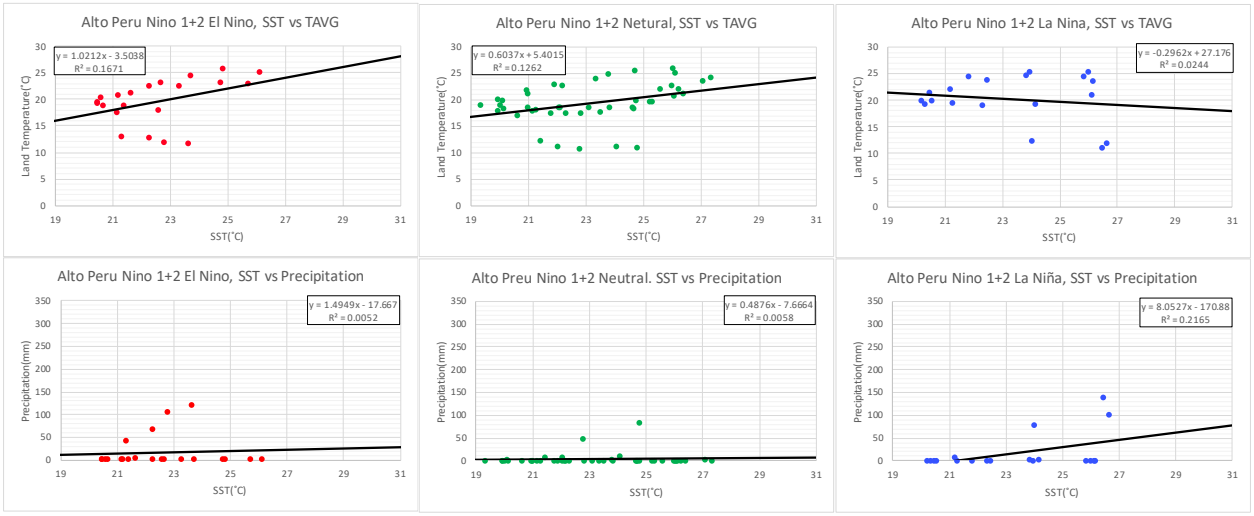

Figure 21

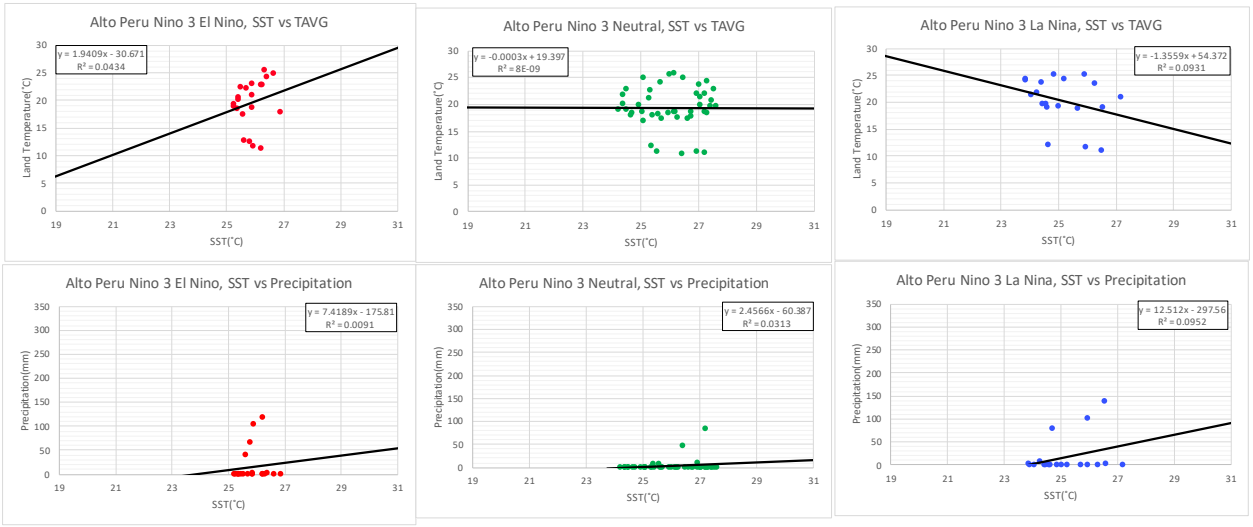

Figure 22

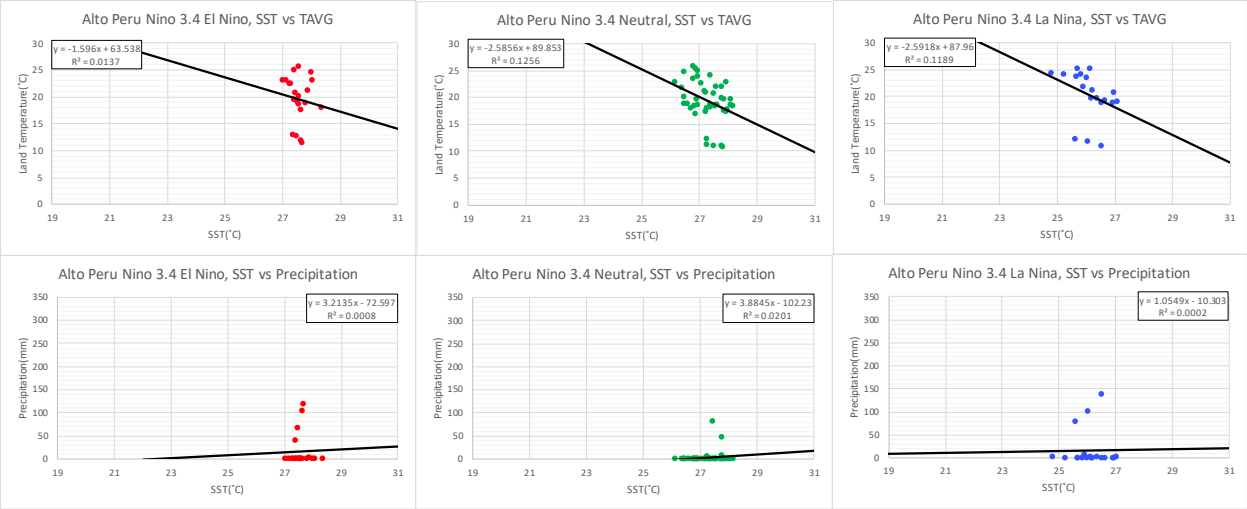

Figure 23

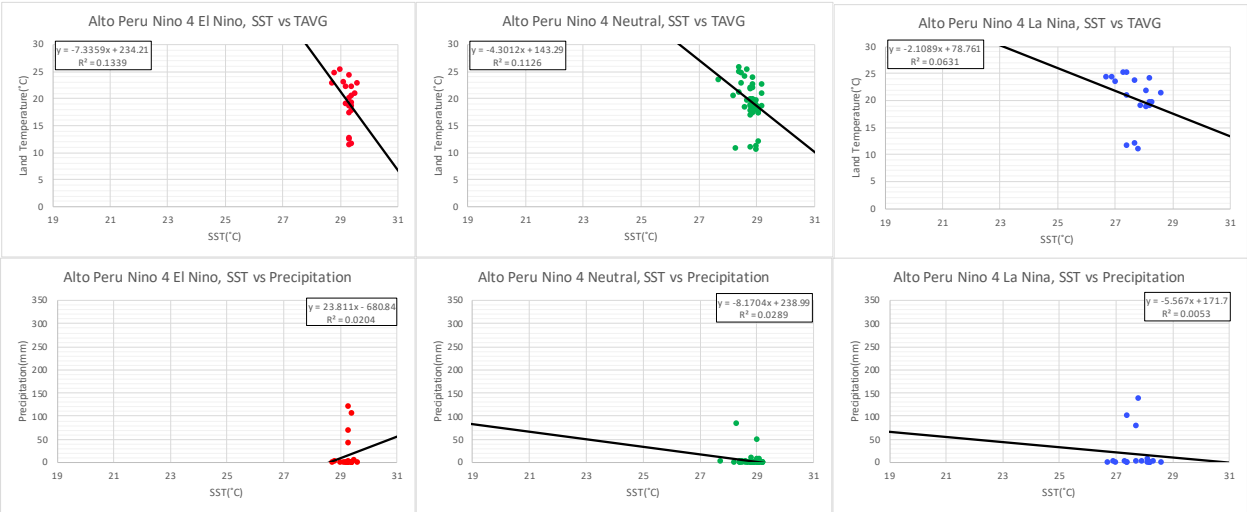

Figure 24

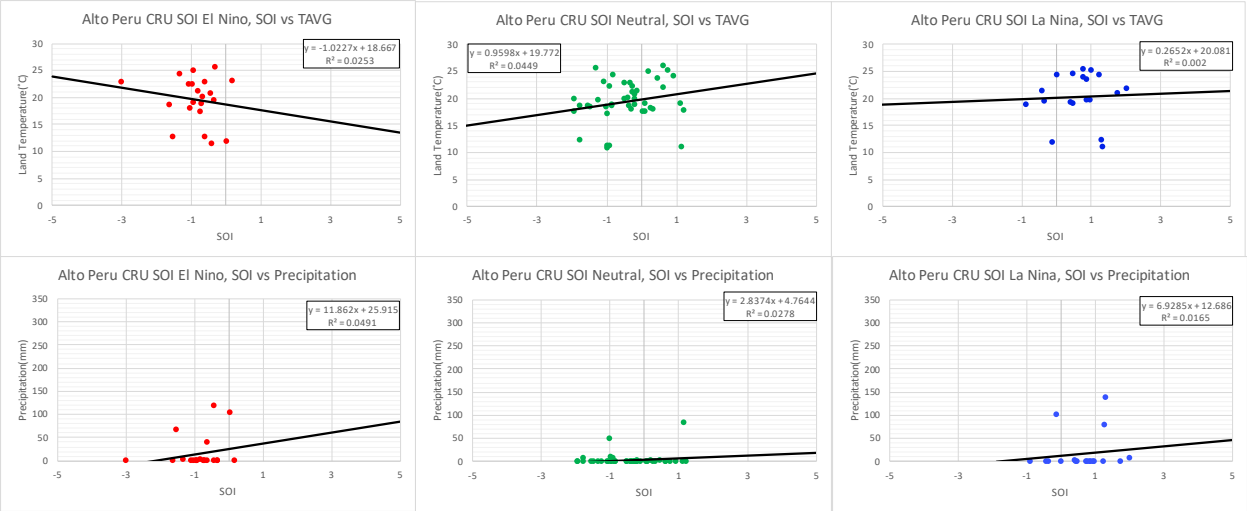

Figure 25

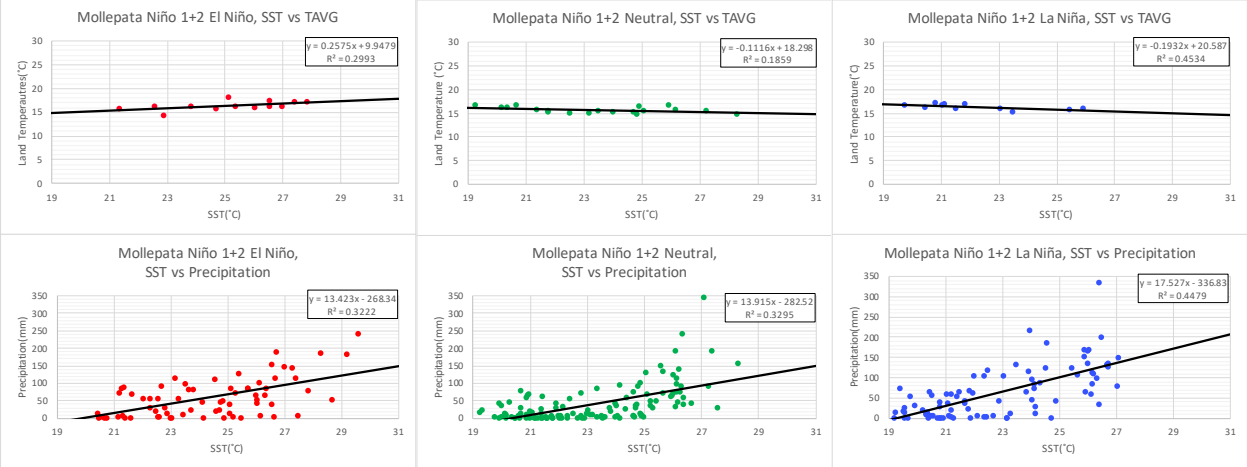

Figure 26

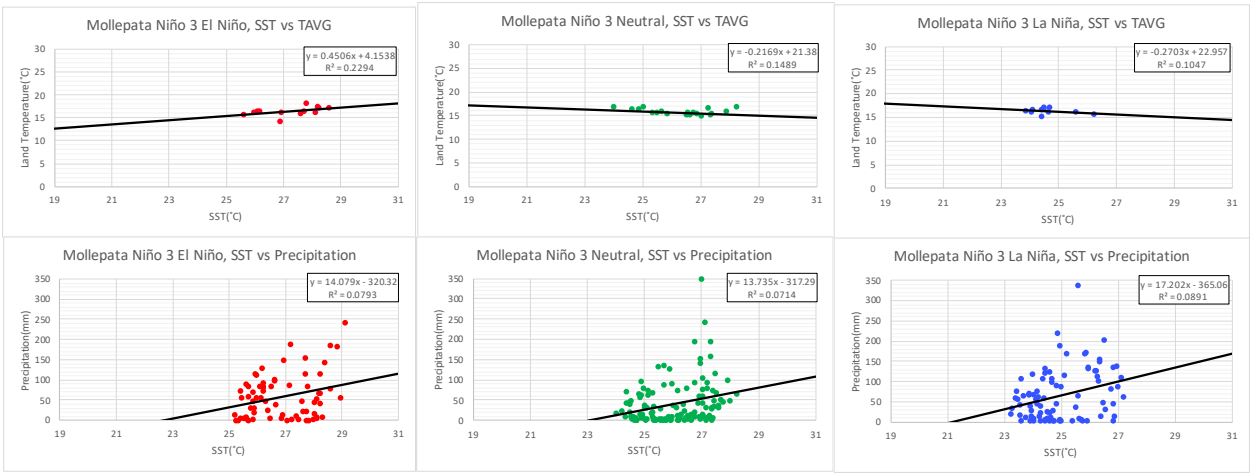

Figure 27

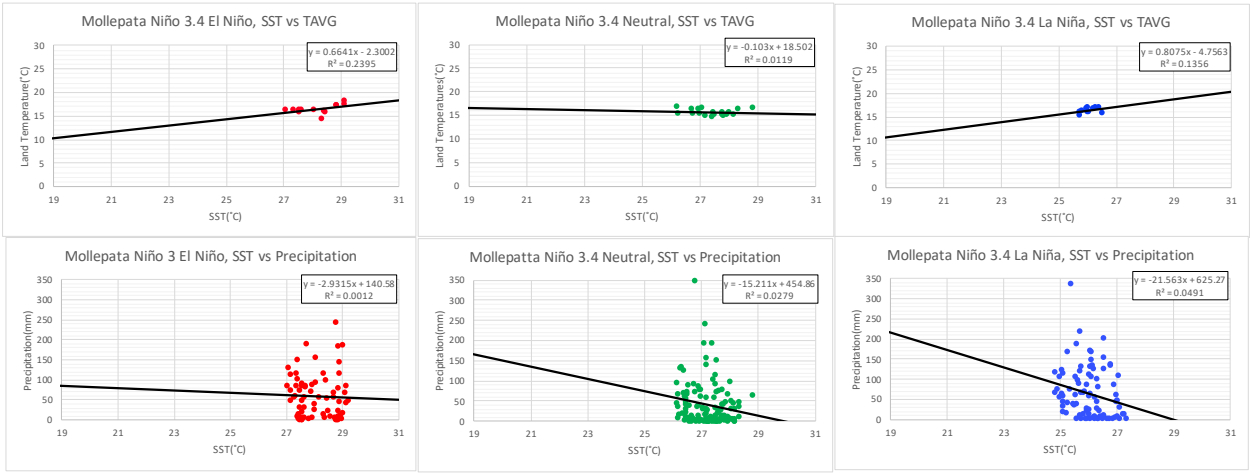

Figure 28

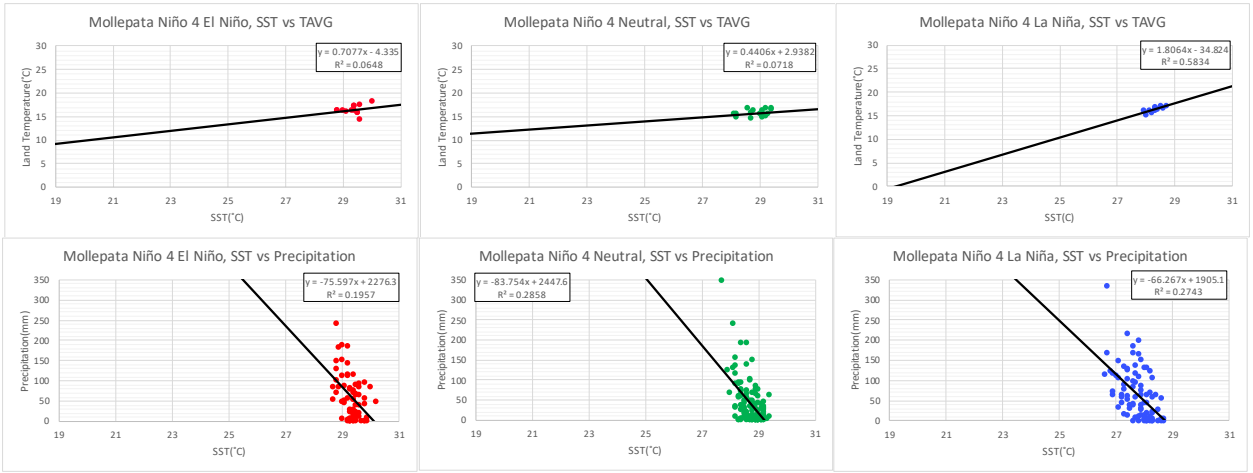

Figure 29

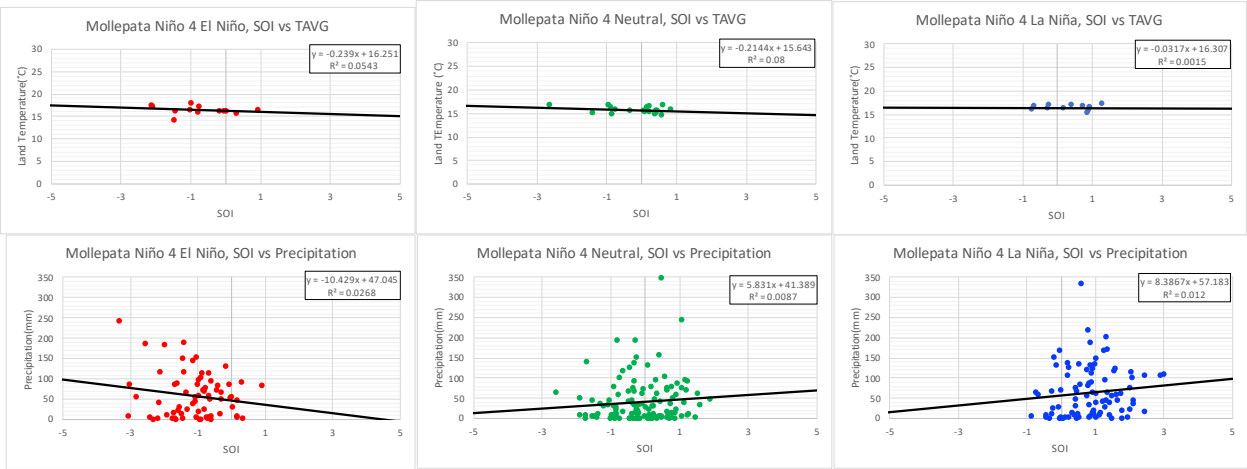

Figure 30

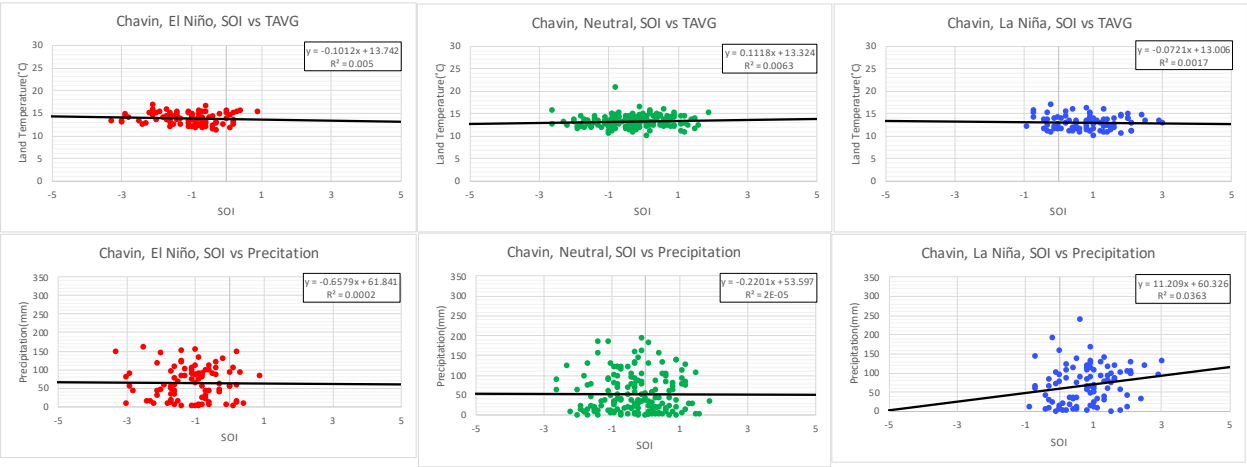

Figure 31

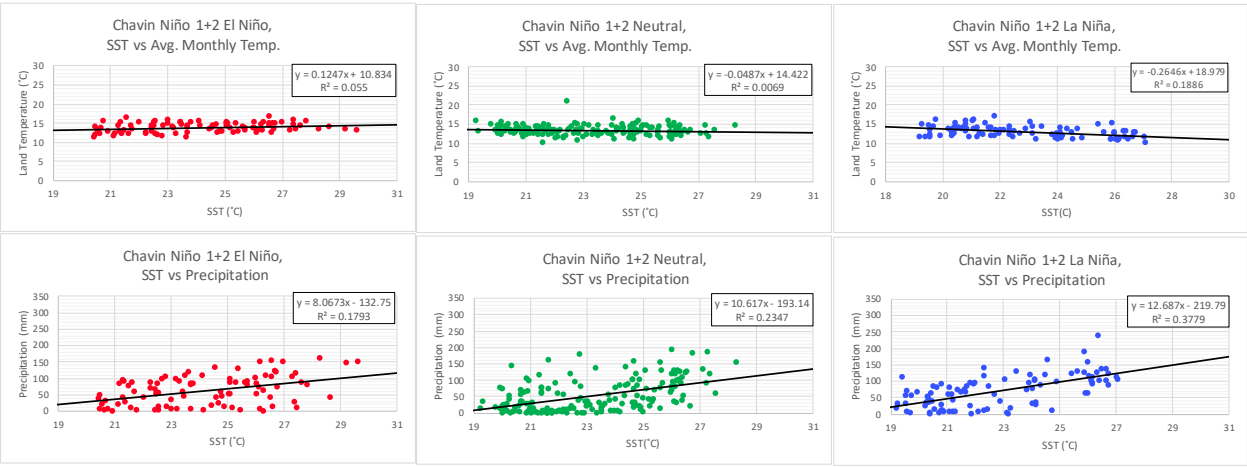

Figure 32

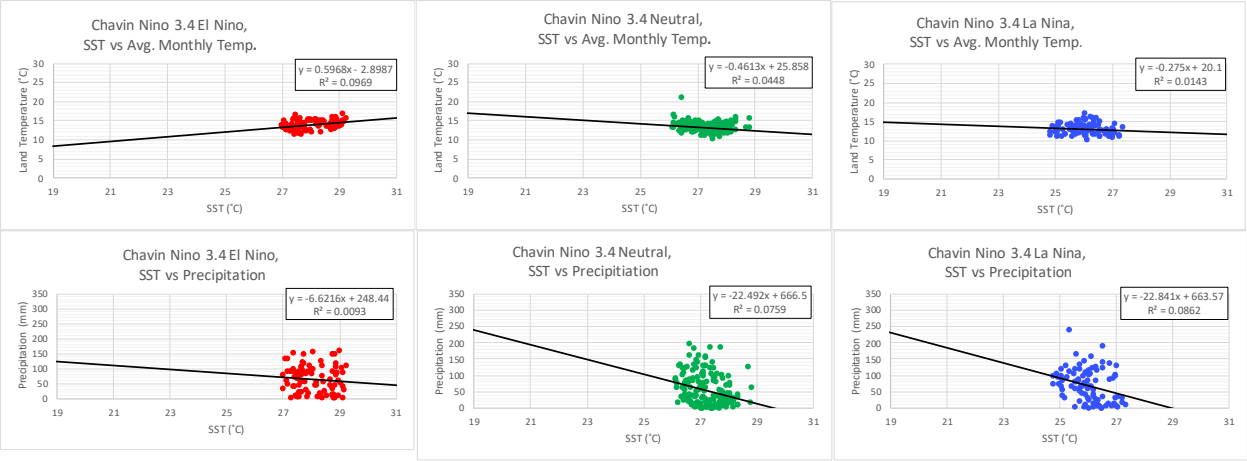

Figure 33

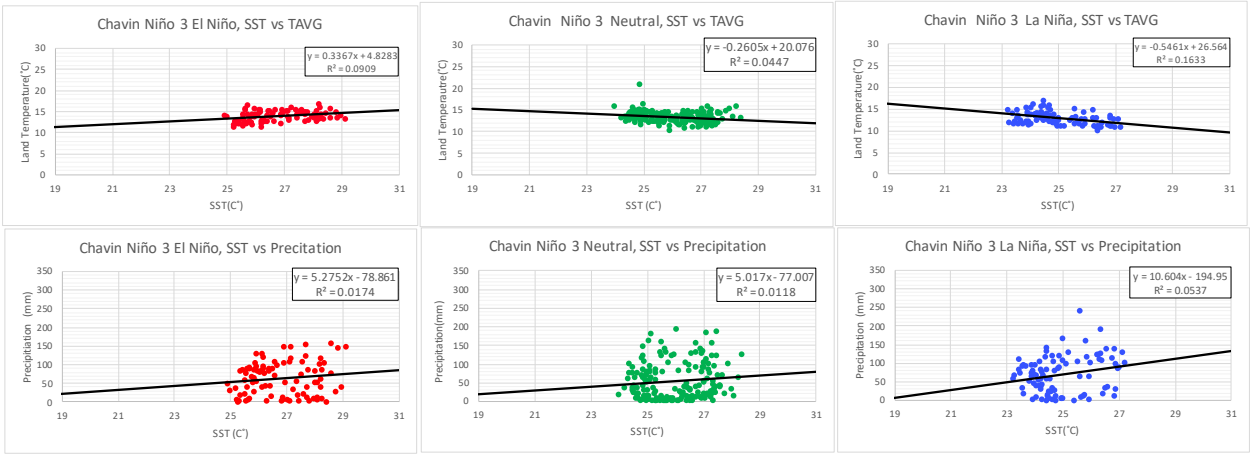

Figure 34

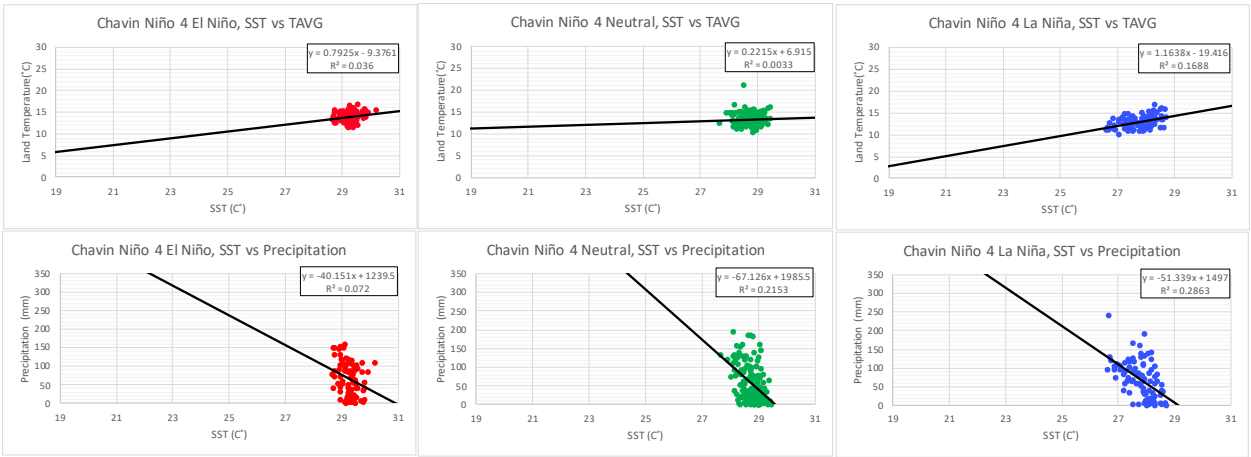

Figure 35

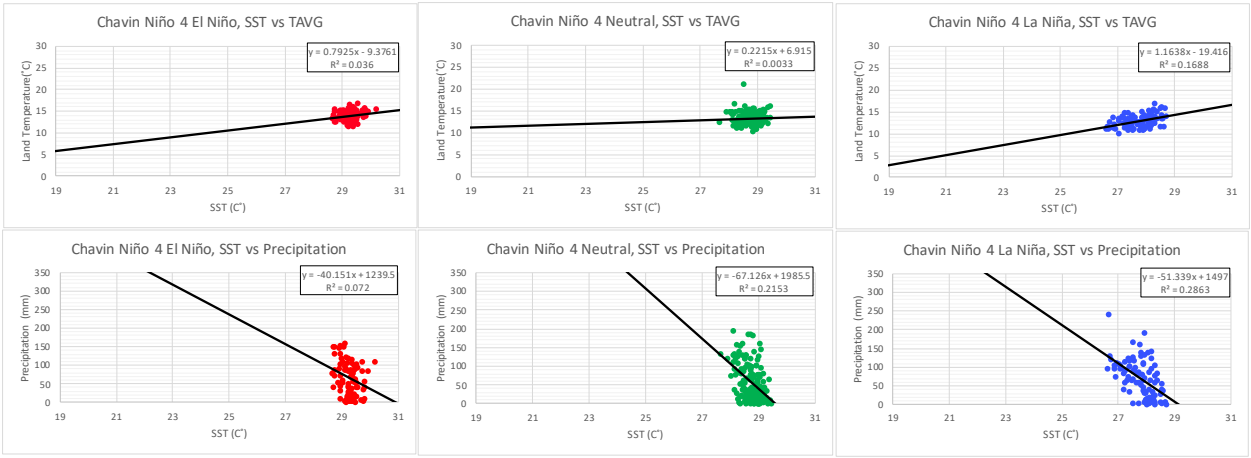

Figure 36

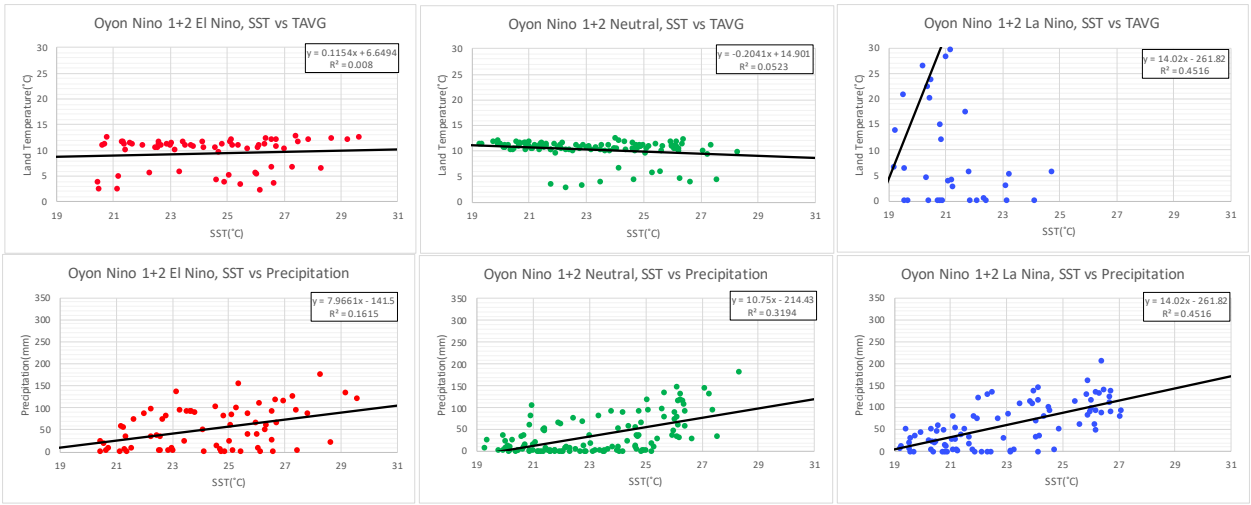

Figure 37

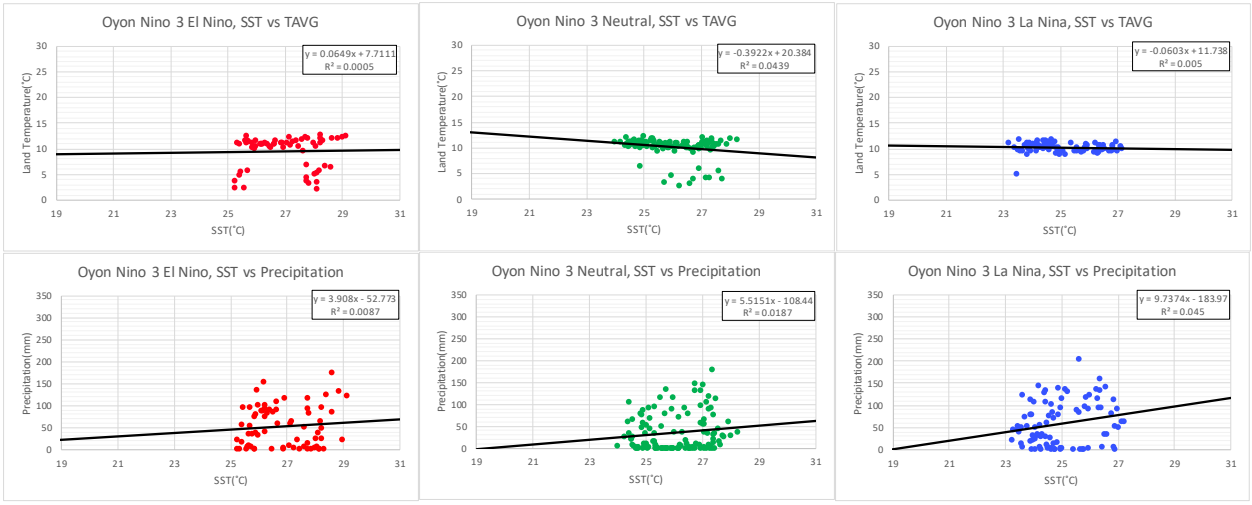

Figure 38

Figure 39

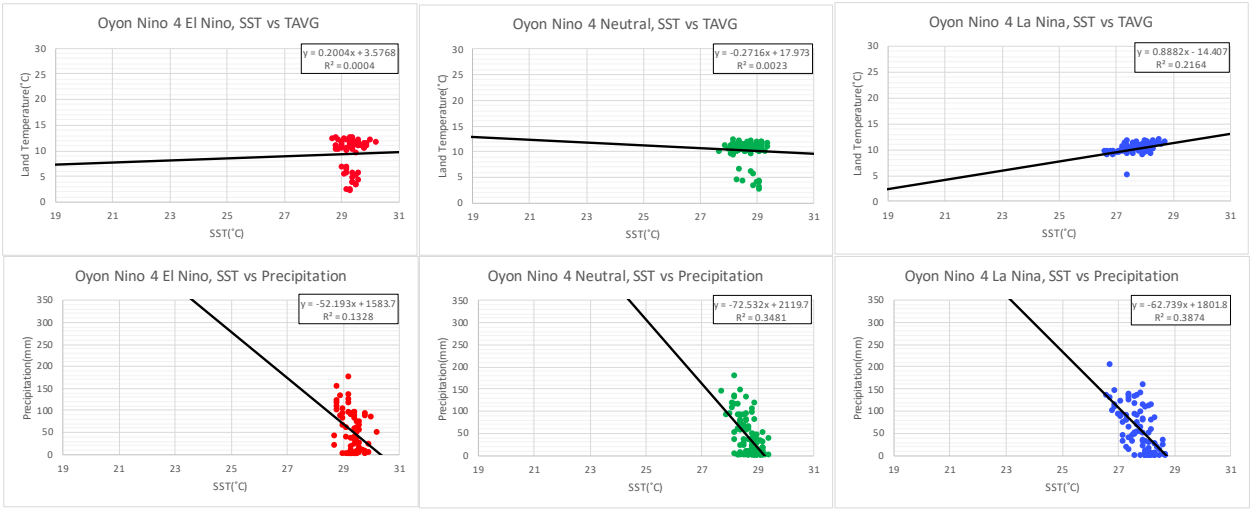

Figure 40

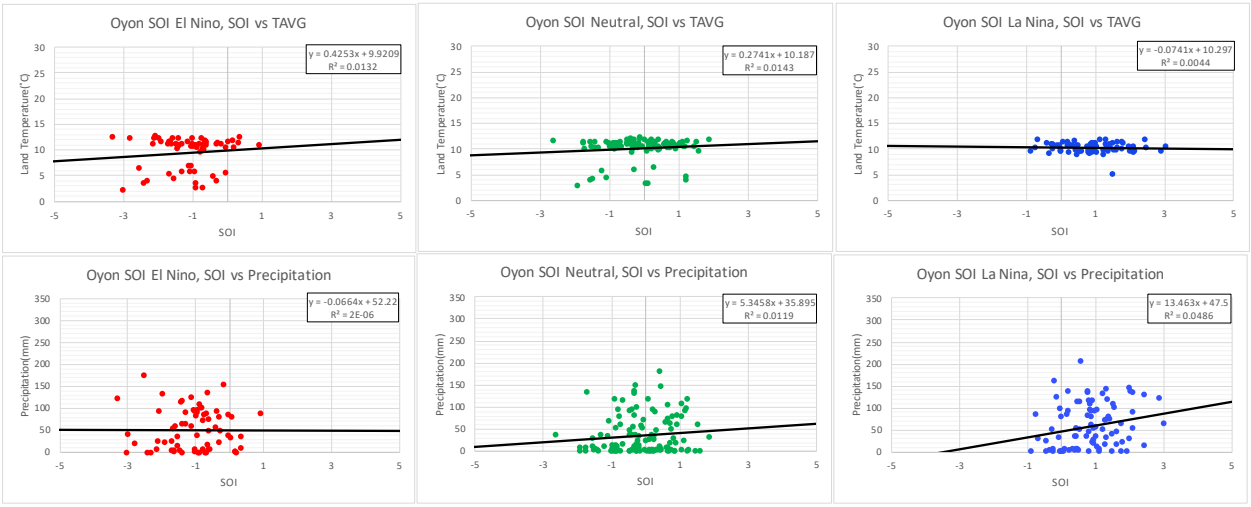

Figure 41

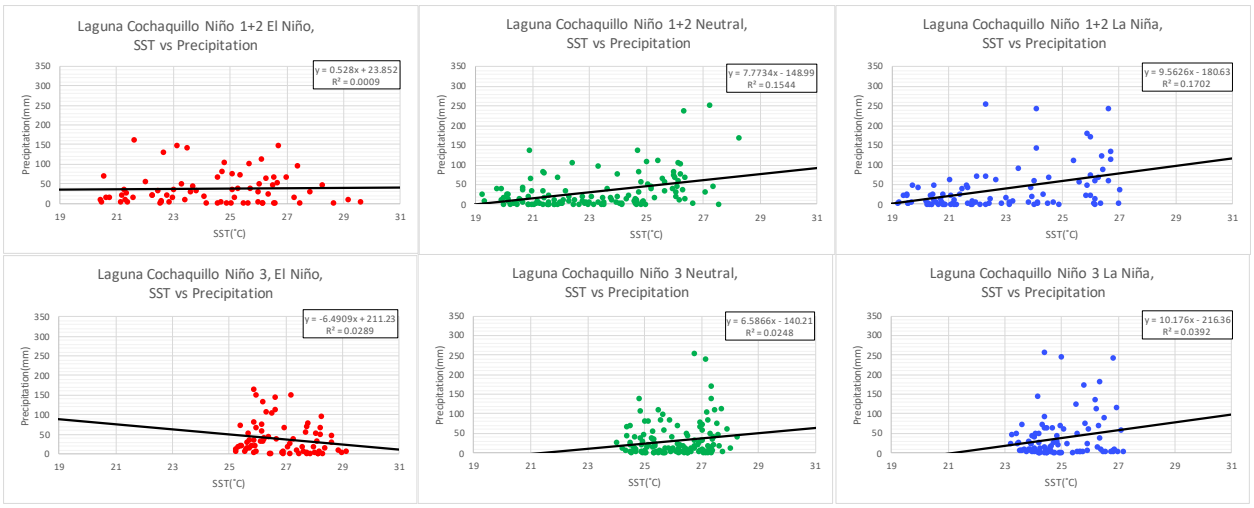

Figure 42

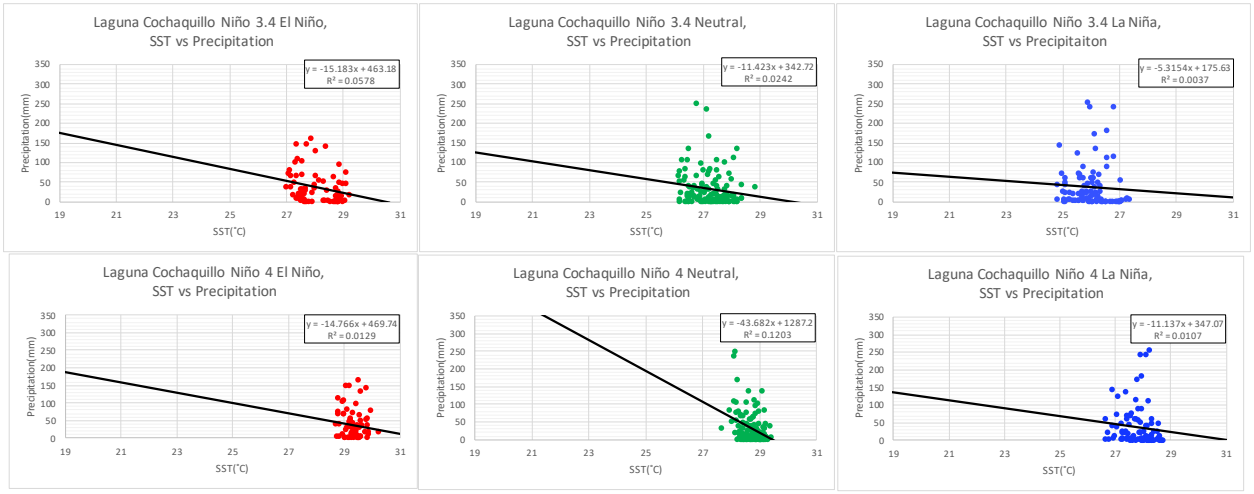

Figure 43

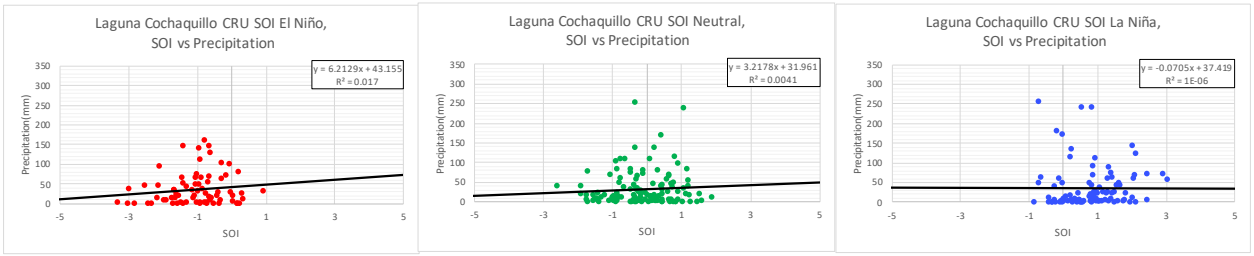

Figure 44